Eur. Phys. J. D **24**, 181–184 (2003)
DOI: 10.1140/epjd/e2003-00104-y

THE EUROPEAN PHYSICAL JOURNAL D

Theoretical study of the time-resolved photoelectron spectrum of Na_2F: effects of thermal initial conditions

M.-C. Heitz[1,a], G. Durand[1], F. Spiegelman[1], and C. Meier[2]

[1] Laboratoire de Physique Quantique[b], IRSAMC, Université Paul Sabatier, 31062 Toulouse, France
[2] Laboratoire Collisions, Agrégats et Réactivité[c], IRSAMC, Université Paul Sabatier, 31062 Toulouse, France

Received 10 September 2002
Published online 3 July 2003 –

Abstract. The excited state dynamics of the Na_2F cluster initiated by a femtosecond laser pulse is studied considering a thermally excited initial sample. Within a pump-probe set-up, the time-dependent photoelectron spectrum is calculated, which is shown to be a sensitive tool to study intramolecular motion of the cluster. Temperature effects are taken into account through thermal averaging over the time-dependent spectra obtained from different initial vibrational states of the cluster. The nuclear motion upon laser excitation is described by full-dimensional quantum wavepacket propagation using explicit, realistic pump and probe pulses. The characteristic features of the time-resolved photoelectron spectra of the Na_2F cluster, identified as due to periodic bending motion of the cluster as well as to the excitation of the stretching mode, are found to be robust against increasing vibrational temperature of the cluster beam. This finding is important for possible future experiments.

PACS. 36.40.Mr Spectroscopy and geometrical structure of clusters – 36.40.Sx Diffusion and dynamics of clusters – 82.53.-k Femtochemistry – 82.53.Hn Pump probe experiments with bound states

1 Introduction

Femtosecond pump-probe spectroscopy has proven to be a powerful tool to monitor in real time primary atomic or molecular processes that happen on a femtosecond timescale. In these experiments, a first ultrashort laser pulse initiates the elementary process to be studied, which is detected by a second, time-delayed probe pulse. Among the different detection schemes the most widely used are based on fluorescence, transient absorption or ionization. Even more detailed information can be gained, if the pump-probe technique is combined with the detection of the energy resolved photoelectron spectrum, as was first proposed theoretically by Seel and Domcke [1]. Until now, it has been applied to a great number of systems, including (polyatomic) molecules or clusters [2].

In this paper we present theoretical simulations on the time-resolved photoelectron spectrum as a tool to study the ultrafast multidimensional nuclear dynamics of the Na_2F cluster. This cluster is the smallest member of a whole family of alkali-halide clusters, which have been studied intensively both theoretically [3–7] and experimentally [8–10]. But only recently, these clusters have been addressed by ultrafast pump-probe set-ups to open the way to study their dynamics in real time [11,12]. For the first time, the Na_2F cluster dynamics could thus be observed in real time by measuring the total ion yield as a function of delay time between the pump and probe pulse [11]. These results were well reproduced and interpreted by theoretical simulations based on classical trajectories [6,11]. In contrast, in this work, we will focus on the *time* and *energy* resolved electron signal that stems from the interaction of both the pump and probe pulse with the molecular sample. We will especially focus on a possible experimental realization of the proposed set-up. To this end, in order to reliably predict or interpret future experiments, possible initial excitations of the clusters in the source needs to be taken into account. In addition to previous studies based on a pure initial ground state [13], we will show here that even in an ensemble of fairly hot clusters, as typically produced by sources based on laser vaporization [10], the ultrafast cluster dynamics is clearly visible in the time-resolved photoelectron spectrum, which we believe to be an encouraging result for a possible experimental realization.

2 Theory and methods

2.1 Potential energy surfaces

In order to model the potential energy surfaces of the electronic ground state and first excited state of the Na_2F cluster, we use the same one-electron pseudo-potential model that has successfully been employed to study the electronic and structural properties of a wide range of

[a] e-mail: heitz@irsamc.ups-tlse.fr
[b] UMR 5626 du CNRS
[c] UMR 5589 du CNRS

Na_nF_{n-1} clusters [3,4]. Namely, the Na_2F molecule is described as a system of two positive sodium ions, one fluorine anion and a single electron. The two lowest adiabatic potential energy surfaces involved in the photoinduced process are calculated using pseudopotentials with repulsive (Born-Mayer) and Coulomb potentials for the ions and a quantum description of the excess electron *via* electron-Na^+ and electron-F^- pseudopotentials, polarization of the ionic cores as well as electron-core correlation being added perturbatively [3]. The energy of Na_2F^+ is calculated as the sum of the Born-Mayer, Coulomb and core polarization contributions due to the ionic electric field. The parameters of the model (Born-Mayer parameters and effective polarization of the ions) have been adjusted to reproduce *ab initio* reference calculations [13].

2.2 Initial conditions and pump excitation

In what follows, we assume a thermalized cluster source at temperature T. Treating a statistical ensemble within the framework of quantum mechanics requires in principle the use of the density matrix. However, since we assume an initial ensemble which is already thermalized, propagating the density matrix is equivalent to several independent wave packet propagations starting with different initial states, with the observables being averaged over the different initial populations.

In order to describe the laser interaction and the subsequent nuclear dynamics, we perform quantum wave packet propagations ($J = 0$) including realistic pulse parameters like the width or the central wavelength, for different initial vibrational states. The coordinate system chosen consists of the two Na-F distances r_1, r_2 and the Na-F-Na angle θ. Details of the numerical wave packet propagation technique, including pulse excitations, can be found in reference [13]. Prior to the pump-pulse interactions, the initial wavefunctions $\psi_i(r_1, r_2, \theta)$ of the electronic ground state have been determined using a Lanczos diagonalization method. This method yields not only the vibrational ground state but also excited vibrational states, which are necessary to study an ensemble of Boltzmann-distributed initial conditions at finite temperatures.

The pump-pulse excitation within first-order time-dependent perturbation theory yields the excited state wavefunction as (in atomic units) [14]:

$$\psi_e^{(i)}(r_1, r_2, \theta, t) = -\mathrm{i} \int_0^t \mathrm{d}t' \mathrm{e}^{-\mathrm{i}H_e(t-t')} \left(\mu_{eg}\mathcal{E}_{pu}(t')\right) \times \mathrm{e}^{-\mathrm{i}H_g t'} \psi_i(r_1, r_2, \theta, t = 0). \quad (1)$$

In this expression, μ_{ge} denotes the transition dipole moment, which in Condon approximation was considered as constant. For the results presented below, the electric field $\mathcal{E}_{pu}(t)$ was taken to be a Gaussian laser pulse.

Table 1. Properties of the initial vibrational states (see text).

i	(ν_1, ν_2, ν_3)	$E_{vib}^{(i)}$ (eV)	$B_i(T = 300$ K)	$\mathcal{P}_{total}^{(i)}$
0	(0, 0, 0)	0.000	1.00	1.00
1	(1, 0, 0)	0.015	0.57	0.13
2	(2, 0, 0)	0.029	0.32	0.29
3	(3, 0, 0)	0.044	0.18	0.29
4	(0, 1, 0)	0.048	0.16	1.00
5	(0, 0, 1)	0.050	0.15	0.97

2.3 Thermally averaged time-dependent photoelectron spectra (TD-PES)

The excited state dynamics following the pump excitation is described by the moving three-dimensional wavepacket. After a well-defined delay time τ, a probe laser interacting with the sample leads to ionization. If we assume a weak probe pulse, its interaction with the cluster can be described by first order time-dependent perturbation theory. In the case of a probe pulse that is sufficiently short as to neglect the nuclear dynamics during its duration, the TD-PES is simply given by [13]:

$$P_i(E, \tau) \propto \int \left| \mathcal{F}\left(E + (V_I - V_e) - \omega_{pr}\right) \times \psi_e^{(i)}(r_1, r_2, \theta, \tau) \right|^2 \mathrm{d}r_1 \mathrm{d}r_2 \, \mathrm{d}\cos\theta \quad (2)$$

where $\mathcal{F}(\Omega)$ is the Fourier transform of the probe laser pulse profile. In this expression, E is the electron energy, ω_{pr} the central probe laser frequency, V_e and V_I the potential energy surfaces of the first electronic excited state and the ionic ground state, respectively. The index i labels the different spectra originating from different initial states. The experimentally measurable spectrum is then given by a Boltzmann average: $P(E, \tau, T) \propto \sum_i B_i(T)\, P_i(E, \tau)$ where $B_i(T)$ are the Boltzmann factors.

3 Results and discussion

3.1 Initial vibrational states

The results for the ground and the first vibrationally excited states are summarized in Table 1. They are labeled as (ν_1, ν_2, ν_3) were the quantum numbers correspond respectively to the bending, asymmetric stretch and symmetric stretch vibrations. Note, however, that these harmonic quantum numbers are used for labeling only, the calculation is *not* based on a harmonic approximation and is thus valid for any excitation level. The ground state geometry is given by $r_1^{eq} = r_2^{eq} = 3.78$ a.u. and $\theta^{eq} = 106.1°$. Figure 1 shows cuts through the three-dimensional wave functions for the ground state (left panel) as well as for the third bending excitation (3, 0, 0) for illustration (right panel). To show the bending excitation, the contours are shown as functions of r_1 and θ while keeping $r_2 = r_2^{eq}$

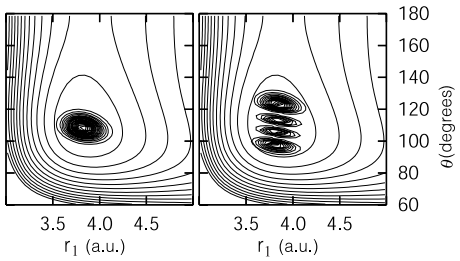

Fig. 1. Contour plots of the ground state (left panel) and third bending (3, 0, 0) excited state (right panel), superimposed on the contours of the electronic ground state potential energy surface for cuts through $r_2 = r_2^{eq}$.

fixed. One clearly sees the nodal structure, indicating the validity of the labeling scheme used for the lowest excited states (Tab. 1). Assuming a thermalized cluster sample of about 300 K, which is a realistic value for cluster sources based on laser vaporization [10], the six states given in Table 1 constitute about 75 per cent of the total population. Note, however, that the different initial states contribute to the final signal not only according to their Boltzmann weights, but also according to the Franck-Condon factors of the pump excitation. It is thus crucial to include this effect, which is correctly taken into account by equation (1). The last column of Table 1 gives, for each initial state, the total population $\mathcal{P}_{total}^{(i)}$ transferred to the first electronic excited state by the pump excitation, relative to the value obtained for the vibrational ground state. The vibrational ground state, the first symmetric stretch and the first asymmetric stretch excited states produce the most efficient excited state population.

3.2 Excited state dynamics

As pump pulse, we used a 40 fs Gaussian laser pulse with a central frequency of 1.02 eV. This pulse induces a resonant transition to the first electronic excited state. The subsequent wave packet motion reflects the ultrafast nuclear dynamics. Since the ground state potential and the first excited state are almost parallel in r_1 and r_2 direction, the laser interaction does not immediately lead to a stretching motion. The situation is entirely different for the bending motion: as can be seen in Figure 2, in the Franck-Condon zone, the excited state potential is strongly repulsive in the θ direction, thus leading to a strong bending motion upon laser excitation. The cluster hence performs a butterfly-like bending motion with a periodicity of 180 fs [13]. These quantum wave packet results confirm studies based on classical trajectories by Hartmann *et al.* [6]. Furthermore, this bending motion has also been observed experimentally [11]. However, due to centrifugal forces, the strong bending motion leads to a slightly delayed symmetric stretch excitation. This behaviour can in some sense be considered as the simplest example of IVR (intramolecular vibrational energy redistribution), a term usually employed in the context of many-mode systems. The excited state quantum dynamics of the Na_2F cluster after femtosecond excitation is described in detail in reference [13].

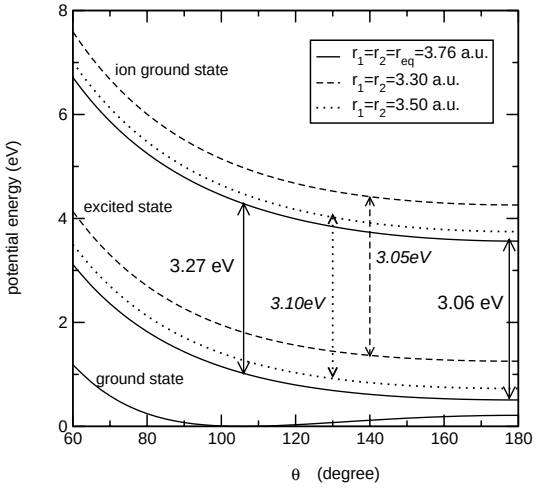

Fig. 2. Cuts through the multi-dimensional potential energy surface along θ for different values $r_1 = r_2$, as indicated, showing the ground state, the excited state and the ionic ground state. The arrows indicate the difference potential between the excited state and the ionic ground state for selected cuts through the potential energy surfaces.

In the following, we will show that the dynamical effects of the bending/stretching coupling is clearly visible in the TD-PES, even assuming a fairly high temperature of 300 K.

3.3 Time-dependent photoelectron spectra

In what follows, we use a Gaussian probe pulse of 3.5 eV center frequency, which allows for ionization of any configuration explored by the nuclear dynamics. A detailed discussion of the theoretical framework for efficiently calculating the TD-PES can be found in reference [13]. As an illustration, Figure 2 shows cuts through the potential energy surfaces for the ground, excited and ionic ground state along θ for fixed $r_1 = r_2 = r_1^{eq}$. The arrows indicate the potential difference between the excited state of the neutral cluster and the ground state of the ion. Since the laser pulses are shorter than the timescale of the nuclear dynamics, we can analyze the ionization process for fixed nuclear geometry, *i.e.* consider the nuclear wave packet to be motionless during the excitation. In this case, the maximum of the kinetic energy distribution of the photoelectrons is given by the probe laser energy minus the difference potential $(V_I - V_e)$ for the nuclear geometry at time τ [15]. In this view, it is clear from Figure 2 that if the probe laser ionizes the cluster at a delay time τ when the cluster geometry is close to linear, we expect electrons with a higher kinetic energy than in the case of the bent geometry. However, this one-dimensional picture is oversimplified, since the slight excitation of the symmetric stretch will modify the cuts through the potential energy surface. To be rigorous, one should consider a

multi-dimensional difference potential. To examine the effects of the aforementioned symmetric stretch excitation, in Figure 2 we have added cuts through the potential energy surfaces referring to $r_1 = r_2 = 3.5$ a.u. and 3.3 a.u. The latter value is reached by the moving wave packet at times of maximal stretch excitation around 355 fs and 1067 fs.

In Figure 3 we present examples of the TD-PES corresponding to the initial states depicted in Figure 1, *i.e.* the ground state (left panel) and third bending excitation (middle panel). The right panel shows the full Boltzmann averaged photoelectron spectrum at 300 K including all states from Table 1 with their corresponding weights. The common structure of the TD-PES can be understood with the help of Figure 2: it is clear that the drastic change of the TD-PES during the first 100 fs directly reflects the bending motion of the excited cluster. For longer times, when the cluster passes the collinear configuration with a periodicity of 180 fs, electrons with a high kinetic energy will be produced. This corresponds to the contours in Figure 3 at 80 fs, 260 fs, 440 fs, 620 fs, 800 fs, 980 fs and 1160 fs. However, the spectrum shows a much richer structure than this simple periodic motion: at 355 fs, and again at 1067 fs, the electron spectrum shifts to high energies, even though the cluster is in a bent configuration at these times. As has been shown in reference [13], inspection of the moving wave packet reveals that this shift is due to the symmetric stretch excitation: at 355 fs and 1067 fs, the mean distances r_1 and r_2 have decreased to about 3.5 a.u. As can be seen from Figure 2, this geometry also produces high energy photoelectrons, when ionized by a probe pulse at exactly this time. The time-dependent photoelectron spectrum thus reveals in a very clear way this weak coupling of the bending mode to the symmetric stretch mode.

Comparing the spectra for the different initial states shows that this feature is very robust to temperature effects. The signature of this intracluster motion is clearly visible in all the TD-PES calculated with the different initial vibrational states. The spectra differ only in small details of their shape, as can be seen from Figure 3 where the middle panel shows the TD-PES originating from the third bending excited state. In this particular case, the TD-PES is enlarged due to the larger extent of the initial wavefunction (see Fig. 1). The main temperature effect is a slight washing out of the signal at large delay times, which is due to small differences in the periodicities for the different $P_i(E, \tau)$ considered. However, as Figure 3 (right panel) shows, this does not play a significant role for delay times up to 1 ps.

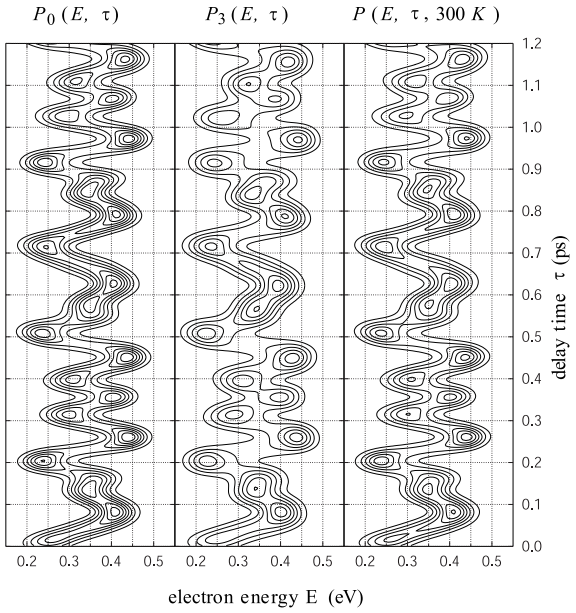

Fig. 3. Time dependent photoelectron spectra for different initial vibrational states (left and middle panel) and Boltzmann averaged signal at 300 K (right panel).

4 Conclusion

In this paper we have investigated the influence of a possible thermal distribution of initial vibrational excitations onto the experimentally observable time-dependent photoelectron spectra. As a main result we can conclude, that up to the relatively high temperatures of 300 K, the clear fingerprint of the bending/stretching coupling is clearly visible. Together with the fact that the presented quantum study employs realistic laser pulse parameters, we believe that the influence of the described bending/stretching coupling on the intracluster dynamics should be experimentally observable.

References

1. M. Seel, W. Domcke, Chem. Phys. **151**, 59 (1991)
2. Special issue of Faraday Discuss. **115** (2000)
3. G. Durand, J. Giraud-Girard, D. Maynau, F. Spiegelmann, F. Calvo, J. Chem. Phys. **110**, 7871 (1999)
4. G. Durand, F. Spiegelmann, Ph. Poncharal, P. Labastie, J.-M. L'Hermite, M. Sence, J. Chem. Phys. **110**, 7884 (1999)
5. V. Bonačić-Koutecký, J. Pittner, J. Koutecký, Chem. Phys. **210**, 313 (1996)
6. M. Hartmann, J. Pittner, V. Bonačić-Koutecký, J. Chem. Phys. **114**, 2106 (2001)
7. G. Durand, F. Spiegelmann, Eur. Phys. J. D **13**, 237 (2001)
8. P. Labastie, J.-M. L'Hermite, P. Poncharal, M. Sence, J. Chem. Phys. **103**, 6362 (1995)
9. P. Poncharal, J.-M. L'Hermite, P. Labastie, Chem. Phys. Lett. **253**, 463 (1996)
10. P. Labastie, J.-M. L'Hermite, Ph. Poncharal, L. Rakotoarisoa, M. Sence, Z. Phys. D **34**, 135 (1995)
11. S. Vajda, C. Lupulescu, A. Merli, F. Budzyn, L. Wöste, M. Hartmann, J. Pittner, V. Bonačić-Koutecký, Phys. Rev. Lett. **89**, 213404 (2002)
12. J.-M. L'Hermite *et al.*, to be published
13. M.-C. Heitz, G. Durand, F. Spiegelman, C. Meier, J. Chem. Phys. **118**, 1282 (2003)
14. C. Meier, V. Engel, *Femtosecond Chemistry*, edited by J. Manz, L. Wöste (Wiley–VCH, Weinheim, 1995)
15. M. Braun, C. Meier, V. Engel, J. Chem. Phys. **103**, 7907 (1995)